The Missing Heme Spin State and a Model for Cytochrome *c'*. The Mixed $S = 3/2, 5/2$ Intermediate Spin Ferric Porphyrin: Perchlorato(*meso*-tetraphenylporphinato)iron(III)

Christopher A. Reed,*[1] Toshio Mashiko,[1] Steven P. Bentley,[1] Margaret E. Kastner,[2] W. Robert Scheidt,*[2] K. Spartalian,[3] and George Lang*[3]

Contribution from the Departments of Chemistry, University of Southern California, Los Angeles, California 90007, and University of Notre Dame, Notre Dame, Indiana 46556, and the Department of Physics, Pennsylvania State University, University Park, Pennsylvania 16802. *Received November 8, 1978*

Abstract: The uncommon d^5 intermediate spin state is found in a series of *meso*-tetraphenylporphyrinatoiron(III) complexes of general formula Fe(Y)(TPP) where Y is a so-called weak ligand (ClO_4, BF_4, PF_6, SbF_6, and CF_3SO_3). Synthesis is achieved by AgY metathesis with FeCl(TPP). The spin state is characterized by magnetic moments in the range $\mu_{eff} = 4.5$–5.3 μ_B at 300 K. Detailed studies on the perchlorato derivative further characterize the spin state with a somewhat curved Curie-Weiss plot (4–300 K), Mössbauer data ($\Delta E_q = 3.5$, $\delta = 0.38$ mm s^{-1} at 4.2 K), solid-state ESR ($g_\perp = 4.75$), and a single-crystal X-ray structure on the 0.5*m*-xylene solvate of $Fe(OClO_3)(TPP)$. Crystal data follow: monoclinic, $a = 14.736$ (3) Å, $b = 15.519$ (3) Å, $c = 17.506$ (3) Å, $\beta = 95.17$ (1)°; space group $P2_1/n$; $Z = 4$; $\rho_{calcd} = 1.378$, $\rho_{obsd} = 1.379$ g/cm^3. The perchlorato ligand is monodentate with an unusually short Fe–O distance (2.029 (4) Å). The average Fe–N bond distance is 2.001 (5) Å with the iron(III) atom displaced by an intermediate amount (0.3 Å) from the porphyrin plane. These dimensions are significantly shorter than those of high-spin five-coordinate ferric porphyrins and are consistent with depopulation of the $d_{x^2-y^2}$ orbital. The solid-state $g_\perp = 4.75$ value together with the magnetic moment, which is greatly in excess of the $S = 3/2$ spin-only value, is interpreted in terms of a quantum mechanically mixed $S = 3/2, 5/2$ state remarkably similar to that of certain low-temperature cytochromes *c'*. Investigation of the solution behavior of $Fe(OClO_3)(TPP)$ by NMR, ESR, Mössbauer, and visible spectroscopy, however, suggests that a predominantly high-spin species exists in the solution phase. The relevance of axial ligand field strength changes to hemoprotein structure and spin state is discussed with particular reference to the histidine of the cytochromes *c'*. That a perchlorate ligand causes an intermediate spin complex while chloride, bromide, alkoxide, azide, etc., form high-spin ferric porphyrin complexes leads to the conclusion that perchlorate can be a weaker field ligand than previously supposed, despite relatively good binding. Qualitative crystal field arguments to rationalize the spin state require an interesting compensating dependence of the equatorial ligand field of the porphyrin upon that of the axial ligand.

Introduction

Nature's elaboration of the fundamental iron porphyrin structure has resulted in a multiplicity of functions for the hemoproteins. Thus oxygen transport in the hemoglobins, electron transport in the cytochromes *c*, and oxygen redox chemistry in the cytochromes P_{450} and peroxidases are all achieved at an iron active site by tuning of the parameters which control hemoprotein structure. Protein control of the axial ligation modes of the heme group is one of the most important of these parameters, both number and type being variable. Based on the premise, largely true, that knowledge of the structure of a hemoprotein will reveal much of how it works, the overall objective of our research is to apply the synthetic analogue approach to resolving structural questions about the hemoproteins. The definitive characterization of protein-free heme complexes, which are frequently amenable to more detailed scrutiny than the hemoproteins themselves, provides a structural framework for understanding the changes of spin state and oxidation state in the hemoproteins. Thus all possible spin states for *ferrous* hemes ($S = 0, 1, 2$) have been well characterized in Fe(1-MeIm)$_2$(TPP),[4] Fe(TPP),[5] and Fe(2-MeIm)(TPP)·C_2H_5OH,[6] respectively (TPP = dianion of *meso*-tetraphenylporphyrin).[7] The interplay of oxidation state and axial ligation modes is readily rationalized in terms of ligand field effects on the d-orbital splittings.[8-10] Parallel reasoning can be applied to *ferric* hemes as illustrated in Figure 1. The ubiquitous high-spin $S = 5/2$ state arises in five-coordinate hemes with one moderate to strong field axial ligand (e.g., Fe(SR)(porphyrin),[11] a synthetic analogue for cytochrome P_{450}) or more recently with certain six-coordinate hemes (e.g., $[Fe(R_2SO)_2(TPP)]ClO_4$,[12] a model for aquomethemoglobin). The low-spin $S = 1/2$ state is found only in six-coordinate ferric hemes having two moderate to strong field ligands (e.g., $[Fe(Im)_2(TPP)]Cl$,[13] a synthetic analogue of cytochromes c_3, b_2, and b_5). An intermediate-spin $S = 3/2$ state is expected to arise when a tetragonal field causes one d orbital, namely, the highly antibonding $d_{x^2-y^2}$, whose lobes are directed at the porphinato nitrogen atoms, to be considerably higher in energy than the other four. It appears that so-called weakly coordinating counterions such as perchlorate are ideally suited to this task, and independently both we[14] and Dolphin, Sams, and Tsin[15] have communicated preliminary results on intermediate-spin $S = 3/2$ perchlorato ferric porphyrin complexes. Herein we report the full synthetic details for preparing *meso*-tetraphenylporphyrinatoiron(III) derivatives with a variety of weakly coordinating counterions, the complete X-ray crystal structure of one derivative, $Fe(OClO_3)(TPP)$·0.5*m*-xylene, Mössbauer and magnetic results, and finally an NMR and ESR analysis of their behavior in solution.

The need for definitive studies on intermediate-spin $S = 3/2$ hemes is severalfold. Firstly, Maltempo has discovered that there is a major contribution of an $S = 3/2$ state to the spin state of certain cytochromes *c'* and also to horseradish peroxidase at low temperature.[16,17] Such a so-called quantum mechanically mixed $S = 3/2, 5/2$ state (as distinct from a thermal spin equilibrium) remains unidentified in synthetic hemes and its existence in a cleanly synthesized complex would lend credence to this theoretical rationale. Secondly, it should be pointed out that the quantum mechanical mixing of some quartet state ($S = 3/2$) into the sextet ($S = 5/2$) is the commonly accepted and widely used rationale for lifting the degeneracy of the sextet ground state.[18] This gives rise to the zero-field splitting term $D(S_z)^2$ in the spin Hamiltonian treatment of high-spin ferric

0002-7863/79/1501-2948$01.00/0

hemes. Ground-state $S = 3/2$ systems should provide an important complement to these analyses. Thirdly, we were interested to see whether the stereochemistry of an intermediate-spin heme, particularly the Fe–N distances and the out-of-plane displacement of the iron, would fit rationally into the patterns of stereochemistry found in hemes of related spin states. Fourthly, regardless of any possible biological significance, there is an intrinsic interest in the $S = 3/2$ state because of its uncommon occurrence in the d^5 ferric ion. Of the reported examples[19-22] an instructive set of complexes is provided by tetraaza ferric complexes[19] where the ligand field strength of the planar ligand set is varied by chelate ring size manipulation. The small rings raise the $d_{x^2-y^2}$ orbital energy well above the other four so that the intermediate-spin state is favored over the high-spin state. By contrast in our heme chemistry the same planar ligand (the porphyrin) is retained while the axial ligand is varied. Fifthly, it is of fundamental importance to explore the ligand field strength of coordinated perchlorate, tetrafluoroborate, etc., since these anions are rarely found coordinated. Finally, perchlorate coordination to hemes needed clarification. The original work of Ogoshi[23] on $Fe(ClO_4)(OEP)$ is in conflict with the more recent work of Dolphin et al.[15] in both the identification of the spin state and the assignment of infrared vibrational frequencies for the coordinated perchlorate.

It was also our goal in this research to explore the synthetic utility of the perchlorate counterion. Its infrared fingerprint turns out to be useful in monitoring reactions and its displacement from $Fe(OClO_3)(TPP)$ by water in $[Fe(H_2O)_2(TPP)]ClO_4$[14] and sulfoxides in $[Fe(R_2SO)_2(TPP)]ClO_4$[12] has led to a whole new class of ferric hemes which have proved[24] to be the key to resolving the controversy over core expansion[25] vs. doming[26] in the interpretation of structure-sensitive resonance Raman heme frequencies.

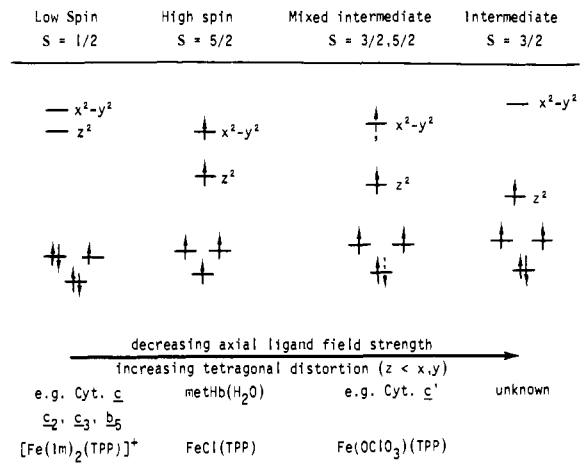

Figure 1. A qualitative representation of the presumed d orbital splittings for the spin states of ferric hemes as a function of axial ligand. The dashed arrows in the mixed intermediate-spin state represent the partial occupancies which arise from an $S = 3/2, 5/2$ admixture; it represents a single spin state, not a spin equilibrium, as described in the text. Below each configuration are hemoprotein and synthetic examples of each spin state.

Experimental Section

Synthesis. As a precaution against hydrolysis with formation of μ-oxo dimer, $[Fe(TPP)]_2O$, all reactions were carried out in dried solvents in a Vacuum Atmospheres Corp. drybox under a He or N_2 atmosphere. Once isolated as crystalline solids all samples were found to be air stable. Solvents were dried and degassed by distillation from sodium/benzophenone except for heptane, which was degassed by bubbling with N_2 and dried over CaH_2. FeCl(TPP) was prepared by an adaptation of a literature method[27] and all other chemicals were of reagent grade. Room temperature magnetic susceptibilities on solids, corrected for diamagnetism, were measured in air on a Cahn 7600 Faraday system and at low temperature on an SCT "squid" system at Stanford University by courtesy of Professors J. P. Collman and R. H. Holm. NMR spectra were run on Varian T60 or XL100 spectrometers. ESR spectra were run at about 10 K on a Varian E12 spectrometer equipped with an Air Products Heli-Tran cryostat with a temperature controller. Mössbauer spectra were obtained as previously described.[12]

$Fe(OClO_3)(TPP)\cdot 0.5C_7H_8$. A mixture of FeCl(TPP) (2.00 g, 2.84 mmol), $AgClO_4$ (2.84 mmol), and THF (120 mL) was boiled gently for several minutes and then filtered through a coarse frit. Heptane (180 mL) was added gradually with continuous swirling and set aside overnight for crystallization. Fine purple crystals of the product were collected by filtration and washed with heptane. Recrystallization was achieved by dissolving the product in a minimum of hot toluene (40–50 mL), filtering through a medium frit, and adding heptane (100 mL). The yield of 0.5toluene solvate was 2.03 g (88%): IR (KBr) νClO_4 1170, 1150, 1120, 840, 610 cm^{-1}; $\mu_{eff} = 5.19\ \mu_B$ (25 °C). Anal. Calcd for $C_{47.5}H_{32}O_4N_4ClFe$: C, 70.08; H, 3.96; N, 6.88. Found: C, 70.51; H, 4.41; N, 6.97. λ_{max}(THF): 400, 526, 658 nm. $g_\perp = 4.75$; $g_\parallel$ 2.03 (solid). Single crystals for X-ray analysis were grown from *m*-xylene and contained 0.5*m*-xylene solvate.

$Fe(OClO_3)(TmTP)\cdot C_7H_8$. This was prepared similarly from FeCl(T*m*TP) and isolated as a toluene monosolvate: IR (KBr) νClO_4 1160–1070, 880, 640–605 cm^{-1}; $\mu_{eff} = 4.5\ \mu_B$. Anal. Calcd for $C_{55}H_{44}O_4N_4ClFe$: C, 72.10; H, 4.84; N, 6.11. Found: C, 71.98; H, 5.42; N, 6.24. λ_{max}(toluene): 411 nm (ϵ 1.22 × 10^5), 514 (1.61 × 10^4), 671. ^1H NMR (toluene-d_8): δ 36 (8 pyrrole), 12 (doublet, 4 meta), 10 (8 ortho), 8.1 (4 para), 2.9 (12 methyl).

$Fe(BF_4)(TPP)\cdot 2C_4H_8O$. This was prepared with $AgBF_4$ in a similar manner except that larger solvent volumes were used and recrystallization was done from THF. Entirely satisfactory carbon elemental analyses were not obtained, possibly because of partial decomposition to fluoride complexes.[28] However, the very close similarity of its magnetic moment and visible spectrum to those of $Fe(OClO_3)(TPP)$ as well as the asymmetry of νB–F in its infrared spectrum leaves little doubt about the identity of the major product. The same comments apply to SbF_6 and PF_6 derivatives below. IR (KBr): νBF_4 1070, 1050 cm^{-1}. $\mu_{eff} = 5.1\ \mu_B$ (25 °C). Anal. Calcd for $C_{52}H_{44}N_4O_2BF_4Fe$: C, 69.45; H, 4.93; N, 6.23. Found: C, 68.56; H, 4.86; N, 6.23. λ_{max}(THF): 404, 495 sh, 522, 635 nm.

$Fe(PF_6)(TPP)\cdot 5C_4H_8O$ was prepared as above: IR (KBr) νPF_6 830 br, 550 cm^{-1}; $\mu_{eff} = 5.2\ \mu_B$ (23 °C). Anal. Calcd for $C_{64}H_{68}N_4FeP-F_6O_5$: C, 65.47; H, 5.84; N, 4.77. Found: C, 64.88; H, 5.23; N, 4.64. λ_{max}(THF): 402, 505, 525 nm.

$Fe(SbF_6)(TPP)\cdot 5C_4H_8O$ was prepared as above: IR (KBr) νSbF_6 660 (br) cm^{-1}; $\mu_{eff} = 5.3\ \mu_B$ (25 °C). Anal. Calcd for $C_{64}H_{68}N_4O_5SbF_6Fe$: C, 60.77; H, 5.4; N, 4.43. Found: C, 59.53; H, 5.03; N, 4.46. λ_{max}(THF): 398, 524, 605 nm.

$Fe(OSO_2CF_3)(TPP)$ was prepared as above, using toluene for recrystallization, $\mu_{eff} = 5.4\ \mu_B$. Anal. Calcd for $C_{45}H_{28}O_3N_4F_3SFe$: C, 66.10; H, 3.45; N, 6.85. Found: C, 64.90; H, 3.71; N, 6.85. λ_{max}(toluene): 412 nm (ϵ 1.18 × 10^6), 516 (1.43 × 10^5), 656. IR (KBr): νCF_3SO_3 1340 (s), 1240 (s), 1205 (s), 630 (s) cm^{-1}.

$[Fe(py)_2(TPP)]ClO_4$. A 2% solution of pyridine in toluene (0.8 mL, 0.2 mmol) was added dropwise to a stirring solution of $Fe(OClO_3)-(TPP)\cdot 0.5C_7H_8$ (163 mg, 0.2 mmol) in toluene (20 mL) and the reaction mixture was heated to boiling. The brown solution was filtered through a medium frit and cooled to room temperature. Heptane (70 mL) was added gradually with continuous swirling and the solution set aside. Fine purple needles were collected by filtration and washed with heptane (90 mg, 97% based on pyridine): IR (KBr) νClO_4 1090, 615 cm^{-1}; $\mu_{eff} = 2.07\ \mu_B$ (23 °C). Anal. Calcd for $C_{54}H_{38}O_4N_6ClFe$: C, 70.02; H, 4.14; N, 9.07. Found: C, 69.84; H, 4.17; N, 9.02.

$[Fe(4\text{-}CNpy)_2TPP]ClO_4\cdot 0.5C_7H_8$. A 2% toluene solution of 4-cyanopyridine (0.8 mL, 0.15 mmol) was added in small portions to a solution of $Fe(OClO_3)(TPP)\cdot 0.5C_7H_8$ (163 mg, 0.2 mmol) in toluene (15 mL). After the mixture was stirred for several minutes, a purple precipitate appeared. The reaction mixture was boiled and toluene added until the precipitate redissolved completely. The hot solution was filtered through a medium frit and set aside overnight. The purple, crystalline product was collected by filtration and washed with heptane (60 mg, 74% based on 4-cyanopyridine): IR (KBr) νClO_4 1135, 1090, 620, νCN 2235 cm^{-1}; $\mu_{eff} = 2.18\ \mu_B$ (23 °C). Anal. Calcd for $C_{63}H_{44}O_4N_8ClFe$: C, 70.82; H, 4.15; N, 10.49. Found: C, 70.48; H, 4.47; N, 10.67.

Table I. Atomic Coordinates in the Unit Cell of $FeTPP(OClO_3)$[a]

atom type	coordinates		
	10^4x	10^4y	10^4z
Fe	1934 (1)	1362 (1)	1042 (1)
Cl	3818 (1)	1931 (1)	1950 (1)
N_1	1293 (2)	2310 (2)	429 (2)
N_2	1175 (2)	1623 (2)	1904 (2)
N_3	2229 (3)	215 (2)	1524 (2)
N_4	2424 (2)	943 (2)	83 (2)
O_1	3006 (2)	2115 (2)	1423 (2)
O_2	4251 (3)	1218 (3)	1645 (4)
O_3	4381 (3)	2664 (3)	1960 (3)
O_4	3523 (4)	1743 (5)	2654 (3)
C_{a1}	1444 (3)	2573 (3)	−300 (3)
C_{a2}	666 (3)	2885 (3)	677 (3)
C_{a3}	624 (3)	2333 (3)	1977 (3)
C_{a4}	1266 (3)	1240 (3)	2628 (3)
C_{a5}	2114 (3)	−19 (3)	2272 (3)
C_{a6}	2671 (3)	−468 (3)	1215 (3)
C_{a7}	2902 (3)	185 (3)	−20 (3)
C_{a8}	2476 (3)	1409 (3)	−586 (3)
C_{m1}	349 (3)	2910 (3)	1394 (3)
C_{m2}	1717 (3)	477 (3)	2805 (3)
C_{m3}	3000 (3)	−495 (3)	500 (3)
C_{m4}	2027 (3)	2186 (3)	−768 (3)
C_{b1}	896 (4)	3301 (4)	−509 (3)
C_{b2}	410 (4)	3494 (3)	87 (3)
C_{b3}	371 (3)	2385 (3)	2744 (3)
C_{b4}	775 (4)	1724 (3)	3143 (3)
C_{b5}	2468 (4)	−861 (3)	2419 (3)
C_{b6}	2794 (4)	−1145 (3)	1774 (3)
C_{b7}	3256 (4)	192 (3)	−755 (3)
C_{b8}	3003 (4)	939 (3)	−1088 (3)
C_1	−322 (3)	3589 (3)	1579 (3)
C_2	−42 (4)	4383 (4)	1867 (3)
C_3	−662 (4)	4982 (4)	2081 (3)
C_4	−1559 (4)	4801 (4)	1996 (3)
C_5	−1848 (4)	4025 (4)	1709 (4)
C_6	−1230 (3)	3422 (3)	1494 (3)
C_7	1801 (5)	179 (4)	3629 (3)
C_8	2568 (5)	357 (5)	4082 (4)
C_9	2672 (6)	109 (7)	4845 (4)
C_{10}	2038 (9)	−326 (5)	5121 (5)
C_{11}	1272 (10)	−494 (8)	4726 (6)
C_{12}	1146 (8)	−238 (7)	3932 (5)
C_{13}	3497 (4)	−1279 (3)	278 (3)
C_{14}	3050 (4)	−2034 (4)	94 (3)
C_{15}	3521 (6)	−2747 (4)	−145 (4)
C_{16}	4422 (6)	−2723 (5)	−199 (4)
C_{17}	4878 (5)	−1995 (5)	−8 (4)
C_{18}	4429 (4)	−1257 (4)	234 (4)
C_{19}	2175 (3)	2591 (3)	−1531 (3)
C_{20}	3004 (3)	2969 (3)	−1640 (3)
C_{21}	3149 (4)	3348 (4)	2333 (3)
C_{22}	2458 (4)	3333 (4)	−2926 (3)
C_{23}	1643 (4)	2950 (4)	−2826 (3)
C_{24}	1495 (3)	2585 (4)	−2131 (3)

[a] The numbers in parentheses are the estimated standard deviations.

$[Fe(4\text{-}Acpy)_2(TPP)]ClO_4 \cdot C_7H_8$. This compound was prepared as fine, purple crystals (80%) by the same procedure as $[Fe(py)_2(TPP)]ClO_4$, except that the reaction was performed in 60 mL of toluene and 20 mL of heptane: IR (KBr) νClO_4 1100, 620, νCO 1690 cm^{-1}; $\mu_{eff} = 2.39\ \mu_B$ (26 °C). Anal. Calcd for $C_{65}H_{50}O_6N_6ClFe$: C, 70.82; H, 4.57; N, 7.62. Found: C, 70.64; H, 4.63; N, 7.62.

$\{[Fe(pyr)(TPP)]ClO_4 \cdot C_7H_8\}_n$. This polymeric compound was obtained as fine, purple needles (80%) as above, except that the reaction was performed in 60 mL of toluene and heptane was not added: IR (KBr) νClO_4 1090, 615 cm^{-1}; $\mu_{eff} = 2.05\ \mu_B$ (25 °C). Anal. Calcd for $C_{55}H_{40}O_4N_6ClFe$: C, 70.26; H, 4.29; N, 8.93. Found: C, 69.99; H, 4.51; N, 8.48.

$[FeTPP(1\text{-}MeIm)_2]ClO_4 \cdot THF$. 1-Methylimidazole (90 mg, 1.1 mmol) was added to a solution of $Fe(OClO_3)(TPP) \cdot 0.5C_7H_8$ (326 mg, 0.4 mmol) and the complex was crystallized by adding heptane and setting aside overnight (380 mg, 95% based on Fe): IR (KBr) νClO_4 1085, 620 cm^{-1}; $\mu_{eff} = 1.98\ \mu_B$ (25 °C). Anal. Calcd for $C_{56}H_{48}O_5N_8ClFe$: C, 66.97; H, 4.82; N, 11.16. Found: C, 67.04; H, 4.83; N, 11.38.

$Fe(C_6H_5)(TPP) \cdot THF$. A mixture of Fe(TPP)Cl (70 mg, 0.1 mmol), $AgBPh_4$ (43 mg, 0.1 mmol), and THF (15 mL) was refluxed for 2 h and filtered through a medium frit, and heptane (35 mL) was added. After the mixture was set aside overnight, fine, purple needles were collected by filtration and washed with heptane (30 mg, 37% based on Fe). The yield was not optimized. $\mu_{eff} = 3.67\ \mu_B$ (29 °C). Anal. Calcd for $C_{54}H_{41}ON_4Fe$: C, 79.30; H, 5.05; N, 6.85. Found: C, 79.44; H, 5.00; N, 6.89. λ_{max} (THF): 390 (shoulder), 416, 427 (shoulder), 522 nm. When treated with concentrated HCl, the visible spectrum turned to that of Fe(TPP)Cl.

Solution Magnetic Susceptibility. Application of the Evans NMR method[29] to iron porphyrins requires $>10^{-3}$ M solubility for spectrometers operating in the readily accessible frequency range. To achieve sufficient solubility we employed the *m*-tolyl derivative $Fe(OClO_3)(TmTP)$ rather than the TPP derivative as well as using a supersaturated solution. A hot, saturated toluene solution of the complex was allowed briefly to cool and put into a 3-mm capped tube which itself was inserted into a 5-mm NMR tube containing pure solvent. A 6.1 ± 0.1 Hz splitting of the toluene methyl proton shifts was measured using the expanded scale of a Varian T60 spectrometer operating at 33 ± 2 °C. The inner tube was checked for the absence of crystallization after the measurement and the concentration of complex determined spectrophotometrically after quantitative dilution with dry toluene. Duplicate measurements varied by 1% and the estimated absolute error is 5%.

X-ray Structure Determination. Three different solvates of $Fe(OClO_3)(TPP)$ were subjected to preliminary examination on a Syntex $P\bar{1}$ diffractometer. The first, a benzene solvate, appeared to be monoclinic with $a = 15.16$ Å, $b = 16.50$ Å, $c = 18.69$ Å, and $\beta = 105.9°$. This sample did not scatter well and was not examined further. The second, a hemitoluene solvate, was triclinic with $a = 13.42$ Å, $b = 26.26$ Å, $c = 12.19$ Å, $\alpha = 98.6°$, $\beta = 114.5°$, and $\gamma = 87.3°$ and $V = 3866$ Å^3 with four molecules in the unit cell. A Delauney reduction did not reveal any hidden symmetry. The calculated density, for a cell content of $4[FeClN_4O_4C_{44}H_{28} \cdot \frac{1}{2}C_7H_8]$ is 1.397 g/cm^3; the experimental density is 1.381 g/cm^3. Further investigation of this sample was terminated in favor of the third derivative, which presented a more satisfactory crystallographic problem. The hemi-*m*-xylene solvate of $Fe(OClO_3)(TPP)$ was found to be monoclinic with four molecules per unit cell; the space group is $P2_1/n$. Least-squares refinement of 60 reflections, collected at $\pm 2\theta$, led to the following cell constants (λ 0.710 73 Å): $a = 14.736$ (3) Å, $b = 15.519$ (3) Å, $c = 17.506$ (3) Å, $\beta = 95.17$ (1)°, and $V = 3987$ Å. The calculated density at 20 ± 1 °C for a cell content of $4[FeClN_4O_4C_{44}H_{28} \cdot \frac{1}{2}C_8H_{10}]$ is 1.368 g/cm^3; the experimental density, measured by flotation, is 1.379 g/cm^3.

Intensity data were collected using a crystal with approximate dimensions of 0.6 × 0.4 × 0.2 mm, which was mounted in a thin-walled glass capillary. The θ-2θ scan technique was employed and utilized graphite-monochromated Mo Kα radiation. Variable scan rates (1-8°/min) with scans of 0.6° below Kα_1 and 0.7° above Kα_2 were employed with backgrounds collected at the extremes of the scan for 0.5 times the time required for the scan. Four standard reflections were measured every 50 reflections during data collection to monitor the long-term stability; no significant deviations were noted. Intensity data were reduced and standard deviations calculated as described previously.[30] All data for which $F_o \geq 3\sigma(F_o)$ and $\sin\theta/\lambda \leq 0.648$ Å^{-1} were retained as observed, leading to 5124 reflections (56% of the theoretical number possible) that were used in the solution and refinement of structure. No absorption correction was applied.

The structure was solved by the heavy-atom method[31] and refined by a combination of full-matrix and block-diagonal least-squares techniques.[32] With two *m*-xylene molecules in the unit cell, the solvate must be positioned at an inversion center and be disordered. A different electron density map indicated positions for the six atoms of the *m*-xylene ring and a further electron density calculation located the two methyl groups. The eight atoms of the *m*-xylene group were incorporated into further refinement cycles as a rigid group (D_{6h} symmetry for the ring with C-C = 1.395 Å and C-CH_3 = 1.47 Å). This treatment thus allowed two overlapped orientations of the solvate

Table II. Thermal Parameters in FeTPP($OClO_3$)

atom type	anisotropic parameters[a]						
	B_{11}	B_{22}	B_{33}	B_{12}	B_{13}	B_{23}	B, Å^2 [b]
Fe	3.37 (3)	3.20 (3)	3.17 (3)	0.36 (3)	−0.14 (3)	0.38 (3)	3.2
Cl	4.1 (1)	6.2 (1)	6.0 (1)	−0.6 (1)	−1.3 (1)	0.6 (1)	5.2
N_1	3.2 (2)	3.4 (2)	3.0 (2)	0.5 (2)	−0.1 (2)	0.2 (2)	3.2
N_2	3.6 (2)	3.1 (2)	2.9 (2)	−0.0 (2)	−0.1 (2)	0.2 (2)	3.2
N_3	3.6 (2)	3.0 (2)	3.7 (2)	0.3 (2)	−0.3 (2)	0.3 (2)	3.4
N_4	3.6 (2)	3.1 (2)	3.2 (2)	0.1 (2)	−0.3 (2)	0.2 (2)	3.3
O_1	4.2 (2)	4.3 (2)	6.1 (2)	−0.1 (2)	−1.4 (2)	0.6 (2)	4.6
O_2	6.3 (3)	7.5 (4)	18.1 (6)	2.9 (3)	−0.3 (3)	−0.5 (4)	8.9
O_3	5.1 (2)	7.9 (3)	10.7 (4)	−2.8 (2)	−2.1 (2)	−0.1 (3)	6.8
O_4	12.0 (4)	18.2 (6)	5.1 (3)	−6.1 (4)	−1.4 (3)	2.6 (3)	9.5
C_{a1}	3.8 (3)	3.5 (3)	3.0 (2)	0.5 (2)	0.0 (2)	0.3 (2)	3.4
C_{a2}	3.2 (2)	3.4 (3)	3.8 (2)	0.7 (2)	0.1 (2)	0.6 (2)	3.4
C_{a3}	3.3 (2)	3.4 (3)	3.5 (2)	−0.3 (2)	0.1 (2)	0.1 (2)	3.4
C_{a4}	4.3 (3)	3.3 (3)	3.3 (3)	−0.4 (2)	−0.3 (2)	0.3 (2)	3.6
C_{a5}	4.6 (3)	3.6 (3)	3.8 (3)	0.1 (2)	−0.5 (2)	0.8 (2)	3.9
C_{a6}	3.9 (3)	3.3 (3)	4.4 (3)	0.2 (2)	−0.8 (2)	0.0 (2)	3.8
C_{a7}	3.4 (2)	3.2 (3)	3.8 (3)	0.2 (2)	−0.3 (2)	−0.5 (2)	3.4
C_{a8}	3.5 (2)	3.9 (3)	3.3 (2)	0.1 (2)	−0.0 (2)	−0.3 (2)	3.6
C_{m1}	2.8 (2)	3.0 (2)	3.9 (3)	0.2 (2)	0.1 (2)	0.1 (2)	3.2
C_{m2}	4.7 (3)	3.6 (3)	3.1 (3)	−0.0 (2)	−0.1 (2)	0.2 (2)	3.7
C_{m3}	3.7 (3)	3.1 (3)	4.3 (3)	0.4 (2)	−0.4 (2)	0.1 (2)	3.6
C_{m4}	3.7 (2)	3.4 (2)	3.0 (2)	0.4 (2)	−0.3 (2)	0.2 (2)	3.3
C_{b1}	5.4 (3)	4.9 (3)	4.1 (3)	1.3 (2)	0.7 (2)	1.2 (2)	4.5
C_{b2}	5.0 (3)	4.4 (3)	4.7 (3)	1.8 (2)	0.5 (2)	0.8 (2)	4.4
C_{b3}	3.7 (2)	4.1 (3)	3.7 (2)	−0.4 (2)	0.3 (2)	−0.4 (2)	3.8
C_{b4}	4.8 (3)	4.1 (3)	3.3 (2)	−0.4 (2)	0.4 (2)	0.2 (2)	4.0
C_{b5}	6.1 (3)	3.9 (3)	4.4 (3)	0.5 (3)	−0.6 (2)	0.6 (2)	4.6
C_{b6}	5.8 (3)	2.9 (2)	5.4 (3)	0.7 (2)	−0.6 (2)	0.4 (2)	4.4
C_{b7}	5.0 (3)	3.5 (2)	4.1 (3)	1.0 (2)	0.3 (2)	−0.4 (2)	4.0
C_{b8}	4.8 (3)	4.1 (2)	3.4 (2)	0.5 (2)	0.5 (2)	−0.1 (2)	4.1
C_1	4.0 (2)	3.4 (2)	3.2 (2)	0.2 (2)	0.4 (2)	0.3 (2)	3.5
C_2	4.4 (3)	4.1 (3)	6.6 (3)	0.1 (2)	−0.3 (2)	−0.4 (2)	4.9
C_3	6.7 (4)	4.0 (3)	5.9 (3)	1.2 (3)	−1.1 (3)	−0.5 (3)	5.3
C_4	6.2 (3)	5.1 (3)	4.1 (3)	2.4 (3)	0.8 (3)	−0.2 (2)	4.7
C_5	4.2 (3)	6.1 (3)	6.0 (3)	1.0 (3)	1.1 (2)	−0.1 (3)	5.2
C_6	4.1 (3)	3.9 (3)	4.8 (3)	0.2 (2)	0.8 (2)	−0.2 (2)	4.2
C_7	7.9 (4)	3.9 (3)	3.7 (3)	0.3 (3)	0.1 (3)	0.4 (2)	4.9
C_8	6.9 (4)	11.5 (6)	4.3 (3)	1.8 (4)	0.0 (3)	0.8 (3)	6.9
C_9	10.4 (6)	11.3 (6)	4.8 (4)	2.7 (5)	−2.5 (4)	0.7 (4)	7.7
C_{10}	16.8 (9)	5.7 (4)	5.9 (4)	−3.4 (5)	0.1 (5)	1.9 (3)	7.6
C_{11}	25.8 (12)	16.7 (10)	7.1 (6)	−16.5 (10)	−3.4 (7)	5.2 (6)	9.3
C_{12}	21.8 (10)	16.0 (9)	5.9 (5)	−14.1 (8)	−2.1 (5)	3.4 (5)	9.2
C_{13}	4.6 (3)	3.5 (2)	4.3 (2)	0.9 (2)	0.0 (2)	0.6 (2)	4.0
C_{14}	6.6 (4)	4.0 (3)	5.3 (3)	0.2 (3)	−0.3 (3)	−0.5 (3)	5.2
C_{15}	11.1 (6)	4.1 (4)	5.0 (4)	1.6 (4)	−0.7 (4)	−0.6 (3)	6.0
C_{16}	12.3 (8)	6.2 (5)	4.8 (4)	4.8 (5)	0.4 (4)	0.1 (3)	6.3
C_{17}	7.0 (5)	9.0 (6)	6.6 (4)	4.9 (5)	1.8 (3)	2.1 (4)	6.2
C_{18}	5.9 (4)	4.9 (4)	6.7 (4)	1.0 (4)	0.5 (4)	0.4 (4)	5.7
C_{19}	4.1 (3)	3.1 (3)	3.0 (2)	1.3 (2)	0.1 (2)	0.1 (2)	3.2
C_{20}	4.2 (3)	4.3 (3)	3.7 (3)	1.1 (2)	0.3 (2)	0.2 (2)	4.0
C_{21}	4.4 (3)	4.8 (3)	5.1 (3)	1.3 (3)	1.3 (3)	0.9 (3)	4.5
C_{22}	6.2 (4)	4.9 (3)	3.8 (3)	2.6 (3)	1.4 (3)	1.0 (3)	4.3
C_{23}	5.6 (3)	5.4 (3)	3.2 (3)	1.7 (3)	−0.4 (2)	0.2 (2)	4.4
C_{24}	4.1 (3)	4.9 (3)	3.7 (3)	0.1 (2)	−0.4 (2)	0.2 (2)	4.2

[a] The numbers in parentheses are the estimated standard deviations in the last significant figure. The B_{ij} s are related to the dimensionless β_{ij} employed during refinement as $B_{ij} = 4B_{ij}/a_i^* a_j^*$. [b] Isotropic thermal parameters are calculated from $B = 4[v^2 \det(\beta_{ij})]^{1/3}$.

molecule, one related to the other by the center of symmetry at 0,0,0. Additional refinement, followed by different Fourier syntheses, led to approximate locations of the hydrogen atoms of the porphinato ligand. The hydrogen atom positions were idealized (C–H = 0.95 Å, B(H) = C(H) + 1.0 Å^2) and included as fixed contributors in all subsequent refinement cycles. The refinement was then carried to convergence with anisotropic temperature factors for all heavy atoms except those of the solvate molecule. The final values of the discrepancy indices were $R = \Sigma||F_o|-|F_c||/\Sigma|F_o| = 0.074$ and $R_w = [\Sigma w(|F_o|-|F_c|)^2/\Sigma w(F_o)^2]^{1/2} = 0.077$. The final data/parameter ratio was 10.3; the estimated standard deviation of an observation of unit weight was 2.00.

A final difference Fourier map had the seven highest peaks (heights of 0.8–0.5 e/A^3) associated with the *m*-xylene solvate molecule; the map was otherwise featureless. A listing of the final observed and calculated structure amplitudes (×10) is available (supplementary material). Atomic coordinates and the associated anisotropic thermal parameters in the asymmetric unit of structure are given in Tables I and II. The rigid group parameters and derived atomic coordinates for the *m*-xylene group are given in Table III (supplementary material).

Results and Discussion

Synthesis. Metathesis reactions of FeCl(TPP) with silver salts in dry, noncoordinating solvents provide the most con-

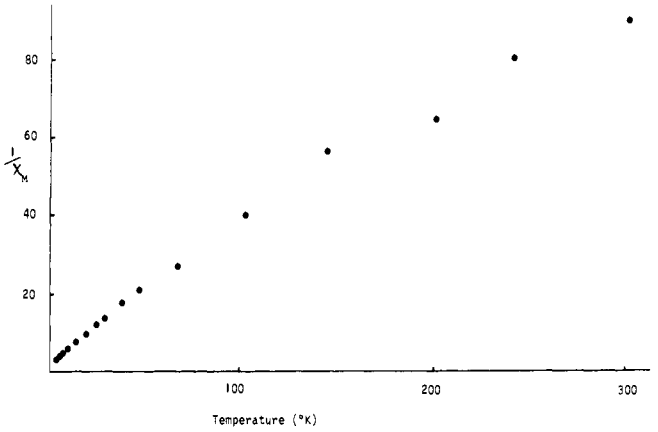

Figure 2. Curie-Weiss plot for the intermediate-spin complex $Fe(OClO_3)(TPP)\cdot 0.5C_7H_8$. The slight curvature is consistent with an $S = {}^3/_2$, ${}^5/_2$ admixture as described in the text.

venient high-yield route to FeY(TPP) derivatives:

$$FeCl(TPP) + AgY \rightarrow AgCl_{(s)} + FeY(TPP) \qquad (1)$$

$$Y = ClO_4, BF_4, PF_6, SbF_6, CF_3SO_3$$

An alternative general route is cleavage of the μ-oxo derivative $[Fe(TPP)]_2O$ with the appropriate acid HY, but the isolation of the desired complexes is complicated by the aqueous medium. High-spin $[Fe(H_2O)_2(TPP)]ClO_4$[12] or $[Fe(C_2H_5OH)_2(TPP)]ClO_4$[33] can arise under certain conditions with perchloric acid; fluoride complexes[28] may contaminate the products from the various fluoro acids. The most well-behaved species is the perchlorate derivative so that most physical measurements have been performed on this derivative. It has higher solubility in organic solvents such as toluene than FeCl(TPP) presumably because of the lack of axial symmetry of the anionic ligand. This solubility immediately suggested perchlorate coordination in solution and this was confirmed by IR in dichloromethane. The intense, broad absorption centered at 1090 cm^{-1} and the strong, sharp band at 620 cm^{-1} of free perchlorate ion in say $[Fe(1\text{-}MeIm)_2(TPP)]ClO_4$ are dramatically split into new bands at 1170 (m), 1100 (m), 880 (m), and 625 (w, br) cm^{-1} in $Fe(OClO_3)(TPP)$. The monodentate coordination found in the solid state by X-ray can be assumed to persist in solution since the vibrational frequencies are similar in both phases. For the BF_4, PF_6, and SbF_6 derivatives coordination is evident in the marked asymmetry of their stretching frequencies on the high-energy side of their major broad absorptions. It is apparent that the drive for electroneutrality in these species is very strong in the absence of donor ligands. All attempts to prepare the planar species $[Fe(TPP)]^+$ or a $[Fe(TPP)(THF)_{1or2}]^+$ cation with a tetraphenylborate counterion have failed and the novel phenyl complex $Fe(C_6H_5)(TPP)$ results. This highlights a major unsolved synthetic problem in chemistry, namely, the preparation of chemically inert, noncoordinating anions as counterions for highly reactive cations. All derivatives crystallize well as purple solids nearly always with accompanying lattice solvates. While searching for a suitable single crystal for X-ray analysis six different crystal modifications of $Fe(OClO_3)(TPP)$ were prepared from benzene, toluene, *p*-xylene, *m*-xylene, THF, and dimethoxyethane. None were shock sensitive, although as a precaution small quantities were used in initial preparations.

In view of Ogoshi's report[23] that various six-coordinate *mono*pyridine adducts of $Fe(OClO_3)(OEP)$ could be prepared we investigated the reactivity of our TPP derivatives toward various donor ligands L. Imidazoles such as 1-methylimidazole or 2-methylimidazole displace perchlorate from $Fe(OClO_3)$-(TPP) giving low-spin ionic complexes of the type $[FeL_2(TPP)]ClO_4$. That 2-methylimidazole gives a low-spin six-coordinate derivative is in contrast to ferrous porphyrins, where only five coordination is stable.[34] The constraints undergone by this complex in forming a six-coordinate low-spin species have been investigated by X-ray single-crystal determination.[35] With pyridines, even using 1 equiv of para deactivated pyridines (such as the *p*-cyano and *p*-acetyl derivatives), only bispyridine adducts were isolated. These results could be interpreted as an expression of the relative solubilities of all the possible products since under situations of fast ligand exchange the least soluble product has the highest probability of crystallizing. However, there is evidence in other closely related ferric hemes that unsymmetrical ligand situations containing one anionic ligand (X) and one neutral ligand (L) in complexes of the type FeXL(porphyrin) are not particularly stable.[11,36] The drive of a ferric porphyrin to attain electroneutrality mentioned earlier with respect to FeY(TPP)-type complexes seems to be well compensated by two N-donor ligands. This is even more curiously illustrated in the isolation of a pyrazine adduct whose low spin state, monopyrazine stoichiometry, and noncoordinated perchlorate (by IR) demand a linear, charged polymeric formulation, $\{[Fe(pyr)(TPP)]\cdot ClO_4\cdot THF\}_n$. We are currently investigating this complex further along with various imidazolate bridged polymeric hemes which are conveniently prepared from $Fe(OClO_3)(TPP)$.[37] Finally, under similar reaction conditions the isolation of adducts with 3,5-dichloropyridine and α-picoline was not observed, presumably for electronic reasons in the former and steric reasons in the latter, although both may be aggravated by unfavorable solubility.

Magnetic Measurements

Interrogation of the ground electronic states of these complexes by a variety of magnetic probes leads at first sight to $S = {}^3/_2$ intermediate spin state assignments in the solid state. Magnetic moments at 25 °C are in the range 4.5–5.3 μ_B consistent with three unpaired electrons. Large orbital contributions to the spin-only moments (3.9 μ_B) would be the simplest explanation of the high values since they are too low for high spin assignments (5.9 μ_B). The situation is reminiscent of intermediate-spin $S = 1$ ferrous porphyrins such as Fe(TPP) which have magnetic moments in considerable excess of their spin-only values.[5] However, the orbital nondegeneracy of the presumed quartet state ($^4A_2$) implies no residual unquenched orbital moment in a moderate magnetic field.[38] The Curie-Weiss plot of $Fe(OClO_3)(TPP)\cdot 0.5C_7H_8$ illustrated in Figure 2 is not strictly linear. The amount of curvature is insufficient to be indicative of a thermal spin state equilibrium but it does suggest that a simple $S = {}^3/_2$ state is an inadequate description of the situation.

Further evidence for the intermediate spin state comes from ESR on solid $Fe(OClO_3)(TPP)\cdot 0.5C_7H_8$ at 10 K, which, although expectedly broad, is remarkably well shaped (Figure 3a). It is a so-called "axial" spectrum with $g_\parallel = 2.03$ and $g_\perp = 4.75$. The $g_\perp$ value is quite different from the $g_\perp \sim 6$ value typical of an axial high-spin ferric heme. Other crystal modifications of the perchlorato derivative as well as the BF_4, PF_6, etc., derivatives all gave solid-state spectra with additional splitting, frequently symmetrical, of the $g_\perp$ signal but all were centered around $g \sim 5$. Simple theory for an $S = {}^3/_2$ ground state would predict $g_\perp = 4$ while relatively straightforward mixing with an energetically close $S = {}^5/_2$ excited state, as put forward by Maltempo,[38] can give rise to g values throughout the range 4–6 according to the amount of $S = {}^3/_2$, ${}^5/_2$ admixture. In fact, the theory developed for the unusual low-temperature $g_\perp = 4.77$ signal of cytochrome *c'* from *Chromatium* is immediately applicable to our derivative with $g_\perp = 4.75$ giving rise to an $S = {}^3/_2$ state with approximately 35% $S = {}^5/_2$ ad-

Table IV. Mössbauer Parameters of Some Intermediate- and High-Spin Ferric Compounds

compd (spin)	T, K	δ,[a] mm s^{-1}	ΔE_q, mm s^{-1}	Γ_1	Γ_2	ref
$Fe(OClO_3)(TPP)\cdot 0.5m$-xylene	4.2	0.38	3.50	0.40	0.33	this
(intermediate)	77	0.38	3.48	0.31	0.28	work
	195	0.34	3.17	0.31	0.29	
	295	0.30	2.79	0.25	0.26	
$Fe(OClO_3)(OEP)$	4.2	0.37	3.57	0.29	0.31	14
(intermediate)	115	0.37	3.52	0.30	0.31	
	295	0.29	3.16	0.27	0.26	
$Fe(C(CN)_3)(TPP)$	78	0.30	3.03	0.35	0.35	74
(intermediate)	298	0.30	3.18	0.44	0.35	
$Fe(Ph_2[15]N_4)(SPh)$	77	0.13	2.55			18
(intermediate)						
$Fe(Me_2SO)_2(TPP)]ClO_4$	4.2	0.45	1.22			12
(high)						
cytochrome c'	4.2	0.34	0.61			67
(high)[b]	4.2	0.37	1.35			
metHb(H_2O)	4.2	0.40	1.3			42
(high)						

[a] Relative to metallic iron. [b] These data refer to the major high-spin component of cytochrome c' from *Rhodospirillum rubrum*. The intermediate-spin component apparently has not yet been studied by the Mössbauer effect.

mixture. Moreover, the magnetic moments which are considerably in excess of the spin-only value for a pure $S = 3/2$ state can be rationalized. Since $g_\perp = 4.75$ for $Fe(OClO_3)(TPP)\cdot 0.5C_7H_8$ essentially determines its magnetic moment at low temperature, the experimental values were compared with those calculated by Maltempo.[38] The agreement is not particularly good ($\mu_{eff}^{4K} = 2.9$, $\mu_{calcd} = 3.5$; $\mu_{eff}^{300K} = 5.18$, $\mu_{calcd} = 4.8$ μ_B) but this should not at this point be taken as a breakdown of the theory since we suspect that the bulk susceptibility data suffers from a serious crystal alignment problem which is difficult to overcome. Moreover, we believe that this problem is widely unsuspected or ignored in measurements of bulk susceptibilities on complexes which are magnetically anisotropic. The serious nature of the problem was discovered during Mössbauer studies. Simply by packing iron porphyrin crystals into a sample holder a nonrandom orientation can frequently be detected, whether the sample is finely ground to a powder or not. Such crystal alignment from packing can give rise to spuriously high or low average magnetic moments in a susceptibility experiment if the anisotropy ($\mu_\perp$ vs. $\mu_\parallel$) is significant. Such anisotropy can be very large for iron porphyrin complexes[39] and we suspect that the present experimental data are lower than the true average μ_{eff} values. Despite the shortcomings in the absolute values the general trend of μ_{eff} as well as the curvature of the Curie–Weiss plot in Figure 2 is in agreement with the theory. One obvious way to overcome this problem is to determine single-crystal anisotropic magnetic moments and such experiments are in progress.[40] We are also experimenting with samples prepared by random suspension in wax since this treatment has solved the problem in Mössbauer effect studies. The additional diamagnetism of the wax and the requirement of its quantitative use, however, pose additional but presumably surmountable problems. It should also be pointed out that in both Mössbauer studies in high magnetic fields and susceptibility measurements in fields as low as 2000g we have observed crystals physically aligning themselves with the field. This gives spuriously high magnetic moments and caution must also be exercised on this count.

Compelling evidence for an intermediate spin state comes from Mössbauer studies where very large quadrupole splittings are apparently quite diagnostic. Preliminary data are listed in Table IV along with comparative literature data on other presumed $S = 3/2$ systems. There is a reasonable resemblance of our TPP derivative to the OEP derivative of Sams et al.[15] In the absence of an applied magnetic field the spectra of

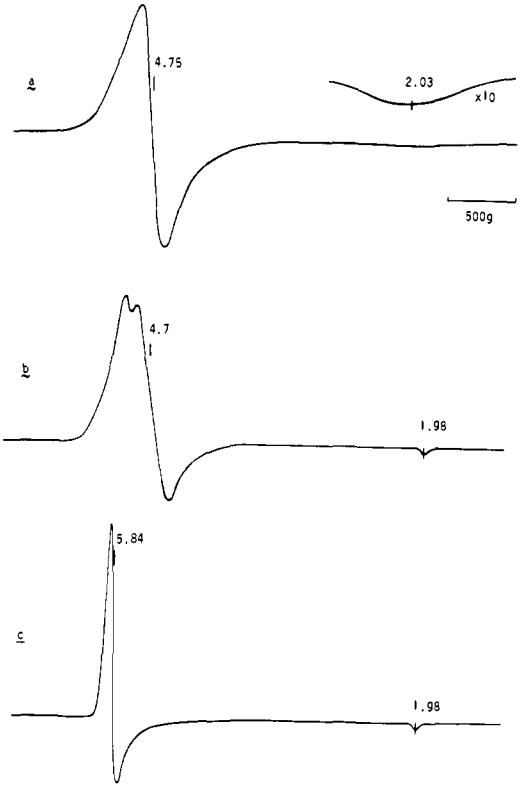

Figure 3. ESR spectra at 10 K of $Fe(OClO_3)(TPP)\cdot 0.5C_7H_8$: (a) in the polycrystalline state; (b) in dry toluene; (c) in 2-methyltetrahydrofuran.

$Fe(OClO_3)(TPP)\cdot 0.5m$-xylene are sharp quadrupole pairs at all temperatures, further establishing that the complex is a magnetically pure, single compound in the solid state. Measurements made in high magnetic fields over the range 4–195 K indicate that the electric field gradient is axial and positive. The magnetic hyperfine interaction exhibits the same symmetry, the internal field being negative and of greatest magnitude when the applied field is transverse to the symmetry axis. The magnitude of this field calculated using Maltempo's mixed spin model[41] is higher than expectations based on values of the magnetic hyperfine coupling constants which are known[42] to apply fairly well to $S = 1/2$ and $S = 5/2$ hemes and hemoproteins. Further theoretical efforts are in progress which

Table V. Bond Lengths in the FeTPP($OClO_3$) Molecule[a]

type	length, Å	type	length, Å	type	length, Å
$Fe-N_1$	2.007 (4)	$C_{a6}-C_{b6}$	1.436 (7)	C_4-C_5	1.358 (8)
$Fe-N_2$	2.000 (4)	$C_{a7}-C_{b7}$	1.431 (7)	C_5-C_6	1.382 (7)
$Fe-N_3$	2.001 (4)	$C_{a8}-C_{b8}$	1.426 (6)	C_1-C_6	1.358 (6)
$Fe-N_4$	1.995 (4)	$C_{a1}-C_{m4}$	1.376 (6)	C_7-C_8	1.350 (8)
$Fe-O_1$	2.029 (4)	$C_{a2}-C_{m1}$	1.379 (6)	C_8-C_9	1.386 (9)
$Cl-O_1$	1.471 (4)	$C_{a3}-C_{m1}$	1.390 (6)	C_9-C_{10}	1.282 (11)
$Cl-O_2$	1.406 (5)	$C_{a4}-C_{m2}$	1.380 (6)	$C_{10}-C_{11}$	1.297 (12)
$Cl-O_3$	1.408 (4)	$C_{a5}-C_{m2}$	1.379 (7)	$C_{11}-C_{12}$	1.440 (11)
$Cl-O_4$	1.375 (5)	$C_{a6}-C_{m3}$	1.383 (7)	C_7-C_{12}	1.314 (10)
N_1-C_{a1}	1.377 (6)	$C_{a7}-C_{m3}$	1.392 (6)	$C_{13}-C_{14}$	1.367 (7)
N_1-C_{a2}	1.382 (6)	$C_{a8}-C_{m4}$	1.399 (6)	$C_{14}-C_{15}$	1.390 (8)
N_2-C_{a3}	1.380 (6)	$C_{b1}-C_{b2}$	1.352 (7)	$C_{15}-C_{16}$	1.339 (10)
N_2-C_{a4}	1.395 (6)	$C_{b3}-C_{b4}$	1.348 (7)	$C_{16}-C_{17}$	1.341 (10)
N_3-C_{a5}	1.385 (6)	$C_{b5}-C_{b6}$	1.340 (7)	$C_{17}-C_{18}$	1.407 (8)
N_3-C_{a6}	1.379 (6)	$C_{b7}-C_{b8}$	1.335 (7)	$C_{13}-C_{18}$	1.383 (8)
N_4-C_{a7}	1.392 (6)	$C_{m1}-C_1$	1.500 (6)	$C_{19}-C_{20}$	1.384 (7)
N_4-C_{a8}	1.384 (6)	$C_{m2}-C_7$	1.508 (7)	$C_{20}-C_{21}$	1.381 (7)
$C_{a1}-C_{b1}$	1.417 (7)	$C_{m3}-C_{13}$	1.490 (7)	$C_{21}-C_{22}$	1.388 (7)
$C_{a2}-C_{b2}$	1.426 (7)	$C_{m4}-C_{19}$	1.510 (6)	$C_{22}-C_{23}$	1.364 (8)
$C_{a3}-C_{b3}$	1.429 (7)	C_1-C_2	1.380 (7)	$C_{23}-C_{24}$	1.379 (7)
$C_{a4}-C_{b4}$	1.422 (7)	C_2-C_3	1.378 (7)	$C_{19}-C_{24}$	1.386 (6)
$C_{a5}-C_{b5}$	1.422 (7)	C_3-C_4	1.346 (8)		

[a] The number in parentheses is the estimated standard deviation in the last significant figure.

Table VI. Bond Angles in the FeTPP($OClO_3$) Molecule[a]

angle	value, deg	angle	value, deg	angle	value, deg
N_1FeN_2	89.2 (1)	$C_{a1}N_1C_{a2}$	105.6 (4)	$N_4C_{a7}C_{m3}$	125.4 (4)
N_1FeN_3	162.2 (1)	$C_{a3}N_2C_{a4}$	105.4 (4)	$C_{b7}C_{a7}C_{m3}$	124.7 (4)
N_1FeN_4	88.7 (2)	$C_{a5}N_3C_{a6}$	105.9 (4)	$N_4C_{a8}C_{b8}$	109.2 (4)
N_2FeN_3	88.7 (2)	$C_{a7}N_4C_{a8}$	105.4 (4)	$N_4C_{a8}C_{m4}$	125.6 (4)
N_2FeN_4	166.1 (1)	FeO_1Cl	131.2 (2)	$C_{b8}C_{a8}C_{m4}$	125.0 (5)
N_3FeN_4	89.1 (2)	$N_1C_{a1}C_{b1}$	109.9 (4)	$C_{a2}C_{m1}C_1$	120.0 (4)
N_1FeO_1	93.9 (1)	$N_1C_{a1}C_{m4}$	125.7 (4)	$C_{a3}C_{m1}C_1$	116.7 (4)
N_2FeO_1	96.1 (2)	$C_{b1}C_{a1}C_{m4}$	124.5 (5)	$C_{a2}C_{m1}C_{a3}$	123.3 (4)
N_3FeO_1	103.9 (2)	$N_1C_{a2}C_{b2}$	110.0 (4)	$C_{a4}C_{m2}C_7$	118.3 (5)
N_4FeO_1	97.8 (2)	$N_1C_{a2}C_{m1}$	126.5 (4)	$C_{a5}C_{m2}C_7$	118.2 (5)
O_1ClO_2	106.7 (3)	$C_{b2}C_{a2}C_{m1}$	123.4 (4)	$C_{a4}C_{m2}C_{a5}$	123.5 (5)
O_1ClO_3	107.2 (3)	$N_2C_{a3}C_{b3}$	109.7 (4)	$C_{a6}C_{m3}C_{13}$	118.8 (4)
O_1ClO_4	107.4 (3)	$N_2C_{a3}C_{m1}$	125.6 (4)	$C_{a7}C_{m3}C_{13}$	118.2 (5)
O_2ClO_3	110.8 (3)	$C_{b3}C_{a3}C_{m1}$	124.7 (5)	$C_{a6}C_{m3}C_{a7}$	123.0 (5)
O_2ClO_4	111.3 (4)	$N_2C_{a4}C_{b4}$	109.8 (4)	$C_{a8}C_{m4}C_{19}$	117.2 (4)
O_3ClO_4	113.1 (4)	$N_2C_{a4}C_{m2}$	125.1 (4)	$C_{a1}C_{m4}C_{19}$	119.5 (4)
FeN_1C_{a1}	127.3 (3)	$C_{b4}C_{a4}C_{m2}$	125.0 (4)	$C_{a1}C_{m4}C_{a8}$	123.3 (4)
FeN_1C_{a2}	126.9 (3)	$N_3C_{a5}C_{b5}$	109.7 (5)	$C_{a1}C_{b1}C_{b2}$	107.9 (5)
FeN_2C_{a3}	127.2 (3)	$N_3C_{a5}C_{m2}$	126.2 (5)	$C_{a2}C_{b2}C_{b1}$	106.7 (5)
FeN_2C_{a4}	125.8 (3)	$C_{b5}C_{a5}C_{m2}$	124.1 (5)	$C_{a3}C_{b3}C_{b4}$	107.7 (4)
FeN_3C_{a5}	126.2 (3)	$N_3C_{a6}C_{b6}$	109.2 (5)	$C_{a4}C_{b4}C_{b3}$	107.4 (4)
FeN_3C_{a6}	127.6 (3)	$N_3C_{a6}C_{m3}$	126.5 (5)	$C_{a5}C_{b5}C_{b6}$	107.7 (5)
FeN_4C_{a7}	127.6 (3)	$C_{b6}C_{a6}C_{m3}$	124.2 (5)	$C_{a6}C_{b6}C_{b5}$	107.5 (5)
FeN_4C_{a8}	126.4 (3)	$N_4C_{a7}C_{b7}$	109.8 (4)	$C_{a7}C_{b7}C_{b8}$	106.8 (4)
				$C_{a8}C_{b8}C_{b7}$	108.7 (5)

[a] The numbers in parentheses are the estimated standard deviations in the last significant figure.

together with single-crystal magnetic anisotropy measurements[40] on identical samples can be expected to yield a more complete understanding of the magnetic state of this molecule.

Crystal Structure

Tables V and VI give the individual bond distances and angles in the Fe($OClO_3$)(TPP) molecule. The numbering scheme used is shown in Figure 4, a computer-drawn model of the molecule. Also displayed in Figure 4 are the bond distances in the coordination group. Figure 5 is a formal diagram of the porphinato core which displays the perpendicular displacements (in units of 0.01 Å) of each atom from the mean plane of the 24-atom core.

Figure 4 clearly shows the five-coordinate nature of the complex. The parameters of the coordination group are an average Fe-N bond distance of 2.001 (5) Å[43] and a displacement of the iron(III) atom of 0.30 Å from the mean plane of the 24-atom core and 0.28 Å from the mean plane of the four nitrogen atoms. These coordination group parameters are quite inconsistent with those expected for a high-spin ferric porphyrin. Five coordination is a common geometry for high-spin ferric porphyrins; a total of nine such derivatives have been structurally characterized.[11,44-51] For these derivatives, the average Fe-N bond distance is 2.068 (8) Å and the displacement of the iron atom from the mean plane of the core is 0.50 (6) Å. The large values of these parameters in the five-coordinate high-spin iron(III) porphyrins are generally associated

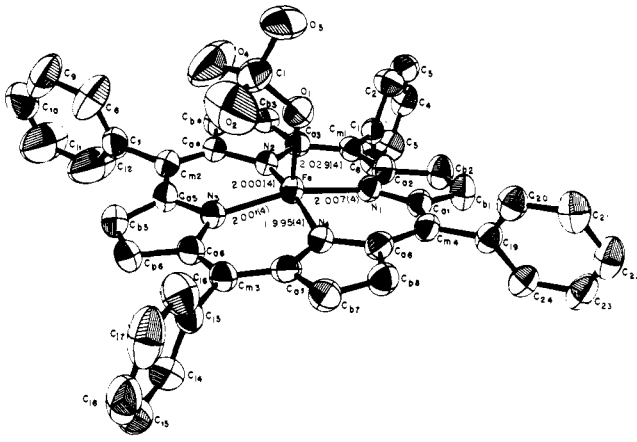

Figure 4. A computer-drawn model of the $Fe(OClO_3)(TPP)$ molecule. The numbering scheme used for the atoms is shown. Also shown are the bond distances of the coordination group.

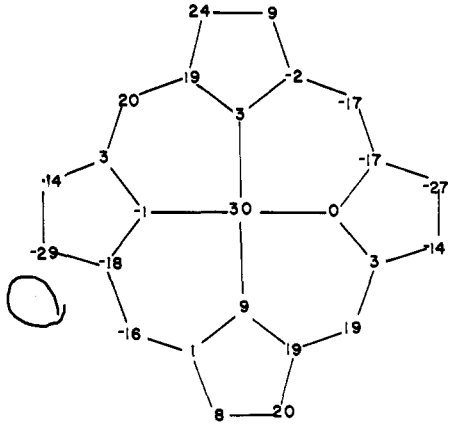

Figure 5. A formal diagram of the porphinato skeleton in $Fe(OClO_3)(TPP)$ showing the perpendicular displacements, in units of 0.01 Å, from the mean plane of core. The core has the same relative orientation as Figure 4.

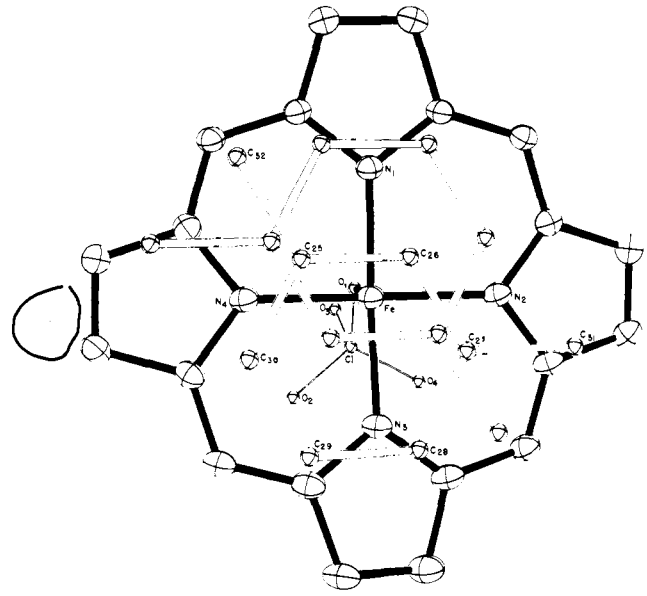

Figure 6. A view of the $Fe(OClO_3)(TPP)$ molecule showing the orientation of the perchlorate ligand and the disposition of the *m*-xylene solvates. The porphinato plane has been rotated 9° out of the plane of the paper; the right-hand side is below the plane.

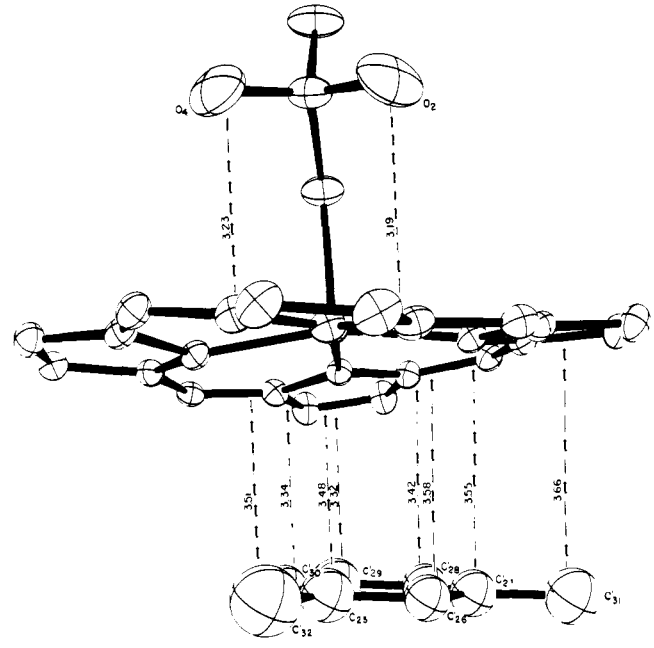

Figure 7. An edge-on view of the interaction between one $Fe(OClO_3)(TPP)$ molecule and the *m*-xylene solvate molecule. Distances shown on the figure are perpendicular distances between the indicated atom and the mean plane of the porphinato core.

with an occupied $3d_{x^2-y^2}$ orbital. Conversely, the Fe–N bond distance of 1.990 (1) Å observed[13,52,53] for low-spin ferric porphyrins is consonant with an unpopulated $3d_{x^2-y^2}$.[8-10] Thus the molecular structure of $Fe(OClO_3)(TPP)$ is clearly inconsistent with a pure high-spin ground state. As discussed previously, the magnetic data for the $Fe(OClO_3)(TPP)$ derivatives are best interpreted as a quantum mechanical admixture of $S = 3/2$ and $5/2$ states. The 0.30-Å displacement of the iron(III) atom might be interpreted in terms of a limited population of the $3d_{x^2-y^2}$ orbital; low-spin five-coordinate cobalt(III) porphyrins[54,55] have metal atom displacements of $\sim 1/3$ this magnitude.

The Fe–O bond distance is 2.029 (4) Å. This bond distance is, to our knowledge, the shortest M–O bond of a perchlorato complex and is presumably the result of highly desirable charge compensation with the porphyrin complex. However, it is quite long in comparison to the Fe–O bond distances of 1.842 (4) Å observed in $Fe(OCH_3)(mesoP)$,[44] the 1.763 (1) Å of $[Fe(TPP)]_2O$,[47] or the 1.752 (1) Å of $[Fe(ODM)]_2O$.[49] The orientation of the perchlorate ligand with respect to the porphinato core is illustrated in Figure 6. The dihedral angle between the FeO_1Cl and N_3FeO_1 planes is 2.1°. A similar orientation of perchlorate is observed in the radical perchlorato(*meso*-tetraphenylporphinato)zinc(II).[56] This bisecting configuration for the perchlorate ligand minimizes nonbonded interactions between uncoordinated oxygen atoms and porphinato core atoms. The closest interatomic separation between the perchlorate oxygen atoms and porphyrin atoms is the 3.35-Å distance between O_2 and N_3. Figure 7 displays the perpendicular distances between the uncoordinated oxygen atoms and the mean plane of the core. All contacts are seen to be larger than the van der Waals radii (1.70 Å for the aromatic ring and 1.40 Å for oxygen). It is thus reasonable to conclude that steric interactions are not responsible for the observed Fe–O bond length. The $FeOCl_1$ angle is 131.2 (2)°; the $Fe–O_1$ vector is tipped ~5° from the normal to the mean plane. Finally, we note that the $Cl–O_1$ distance of 1.471 (4) Å is considerably longer (0.075 Å) than the average Cl–O distance to the uncoordinated oxygen atoms (1.396 (18) Å), consistent with significant electron donation by O_1 to the iron(III) atom.

As is seen from Figure 5, the porphinato core has a ruffled conformation with approximate S_4 symmetry. Deviation from

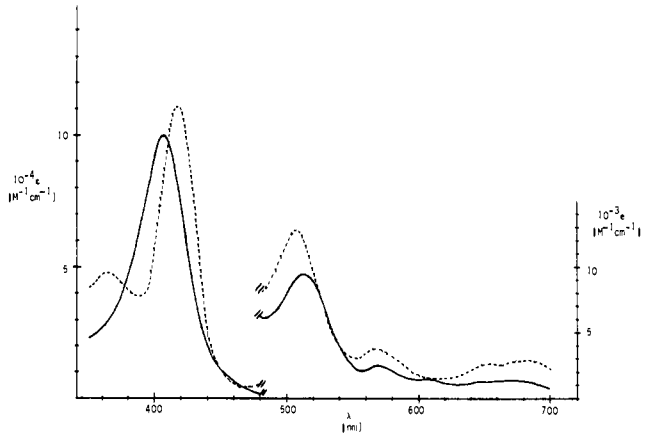

Figure 8. Comparison of the visible spectrum of $Fe(OClO_3)(TPP)$ (—) with that of FeCl(TPP) (---), both in toluene solution.

exact planarity of all phenyl and pyrrole groups is less than 0.01 Å. The dihedral angles between the phenyl groups and the mean plane are 83.5, 78.8, 76.8, and 75.5°.

Agreement between chemically equivalent bond distances and angles in the core is quite satisfactory. Using C_a and C_b to denote the respective α- and β-carbon atoms of a pyrrole ring, C_m for methine carbon, and C_p for a phenyl carbon atom that is bonded to the core, the average bond distances in the core are $N-C_a$ = 1.384 (6) Å, C_a-C_b = 1.426 (6) Å, C_a-C_m = 1.385 (8) Å, C_b-C_b = 1.344 (8) Å, and C_m-C_p = 1.502 (9) Å. Averaged bond angles are $FeNC_a$ = 126.9 (7)°, C_aNC_a = 105.6 (2)°, NC_aC_b = 109.7 (3)°, NC_aC_m = 125.8 (5)°, $C_aC_bC_b$ = 107.5 (6)°, and $C_aC_mC_a$ = 123.3 (2)°. For both sets of averaged values, the number in parentheses is the estimated standard deviation for the averaged value.

The *m*-xylene solvate molecule is located at the center of symmetry at 0,0,0, and has identical geometrical relationships with the two $Fe(OClO_3)(TPP)$ molecules related by this center. The *m*-xylene molecule is disordered. Figure 6 shows the two orientations of the xylene molecules (each related to the other by a center of symmetry and having half occupancy). Their orientations with respect to the porphinato core are also shown in Figure 6. The porphinato and xylene planes are essentially parallel; the angle between the two planes is 5.7°. Similar geometrical relationships between Zn(TPP),[57] Cr(TPP),[58] and Mn(TPP)[59] and toluene molecules of solvation have been reported. A second view of the packing relationships between the xylene solvate and a $Fe(OClO_3)(TPP)$ molecule is given in Figure 7. The perpendicular separations between the eight atoms of the xylene molecule and the porphinato core are also shown; the mean separation is 3.48 Å. There thus appears to be a weak π complex formed between the xylene and the two $Fe(OClO_3)(TPP)$ moieties; the closest distance between iron and a xylene carbon atom is 3.78 Å. The equivalent stoichiometry of the toluene solvate of $Fe(OClO_3)(TPP)$ leads to the real possibility that this derivative also forms a weak π complex involving a solvent molecule and two porphyrin moieties. These observations are consistent with the observed sensitivity of the magnetic state of the iron to its solvation environment.

Other than the packing relationships previously discussed, there appear to be no unusual intermolecular contacts.

Solution Behavior

There is a notable lack of detailed ESR investigations of the $S = 3/2$ systems reported to date[19-22] because of diffuse spectra or poor solubility. We had hoped that the good toluene solubility of the present complexes would allow such a study but this did not turn out to be possible. Instead, mixtures of both high- and intermediate-spin complexes appear to be present in all of our solution-phase measurements.

A typical ESR spectrum at 10 K of $Fe(OClO_3)(TPP)$ in toluene is shown in Figure 3b. The splitting of the $g \sim 5$–6 signal is interpreted as a mixture of distinct high and intermediate spin species rather than a rhombic distortion since an axial spectrum is expected for a pure, single compound.[12] This was observed for one solid sample as discussed earlier. The splitting pattern of $g_\perp$ in toluene is exceedingly variable over the range of FeY(TPP) complexes, while when using 2-methyltetrahydrofuran as solvent the high-spin component ($g \sim 6$) predominates, sometimes exclusively, as illustrated in Figure 3c. In fact, the spectra were so critical on the nature of the solvent that exact reproducibility from one frozen solution to another could not be achieved. Even with vacuum line techniques using toluene that had been very thoroughly dried (using molecular sieves) about 50% of a high-spin component was judged to be present. A Mössbauer spectrum of a frozen toluene solution of the perchlorate derivative showed two quadrupole split doublets again suggesting the presence of two distinct species at low temperature.

At room temperature there are similar observations which speak against the existence of a single intermediate-spin species. Rather, a rapid high-spin/intermediate-spin thermal equilibrium between two components is suggested. (This is not to be confused with the quantum mechanical $S = 3/2, 5/2$ admixture referred to earlier in more accurately describing the electronic state of the single component "intermediate"-spin solid.) Visible spectra of the red-brown complexes in various solvents not only have great similarities with each other but also with the known high-spin FeCl(TPP) as illustrated in Figure 8. The spectrum of $Fe(OClO_3)(TPP)$ in very dry toluene, where the $[H_2O] \ll$ [complex], is essentially identical with that in moderately dry toluene, indicating that six coordination by H_2O is not the likely driving force to the high-spin state. The NMR spectrum of $Fe(OClO_3)(TmTP)$ in dry toluene-d_8 is interesting because its pyrrole proton resonance at 36 ppm downfield from Me_4Si is out of the position diagnostic of high-spin ferric hemes (~80 ppm downfield) as well as that of low-spin hemes (~20 ppm upfield).[72] We consider this chemical shift, which is quite broad (700 Hz), to be an average shift of a high-spin component in rapid equilibrium with an intermediate-spin component since, in the absence of spin density in the $d_{x^2-y^2}$ orbital, the latter component is not expected to have a large downfield shift. Finally, an Evans method magnetic susceptibility on $Fe(OClO_3)(TmPP)$ in toluene at 33 °C gives μ_{eff} = 5.5 μ_B, which is approaching the high-spin value of 5.9 μ_B.

Taken altogether these solution experiments suggest that the ligand field strengths of the coordinating anions are right at the spin crossover point so that very subtle changes in the environment control the spin state. Six coordination by water or donor solvents and aggregation effects may further complicate the solution behavior but we do not favor these explanations. Apparently a single component is favored only in the solid state. Even the 0.5*m*-xylene solvate of $Fe(OClO_3)(TPP)$ differs slightly in its solid state Mössbauer spectrum from the 0.5toluene solvate, again illustrating the sensitivity of the ligand field to its solvation sphere environment.

Field Strength of Perchlorate

That perchlorate is rarely found as a ligand in coordination chemistry means that few opportunities have been found to estimate its ligand field strength. Indications are, however, that it lies very close to chloride in the spectrochemical series.[60,61] The relatively good binding of the perchlorate ion in the present complex as well as the lack of any charge dispersing solvation might lead one to suspect that it could act as a somewhat stronger field ligand than in, say, $[Co(NH_3)_5(ClO_4)]^{2+}$. In

fact, as we will argue in the following discussion, the opposite appears to be true. We believe that ClO_4^-, BF_4^-, PF_6^-, SbF_6^-, and $CF_3SO_3^-$ are very weak field ligands in the present complexes.

We note, first of all, that all other reported five-coordinate ferric heme complexes with a single coordinating anion are *high* spin. In FeX(TPP) these include $X^- = I^-$, Br^-, Cl^-, RS^-, NCO^-, CH_3O^-, $RCOO^-$, N_3^-, and $(O^{2-})_{1/2}$. If the overall spin state of the complex were taken as an indication of the field strength of X (since the TPP remains the same) then one would be forced into the very uncomfortable conclusion that perchlorate is acting as a stronger field ligand than all of the aforementioned. A further frequently quoted, but in this case also misleading, argument which arises naturally from crystal field theory for a tetragonal system[62] is that perturbation of the ligand field in the axial direction (z) should not affect the splitting of d orbitals in the equatorial (x, y) plane. However, since the choice between an $S = 5/2$ and an $S = 3/2, 5/2$ spin state is directly governed by the separation of the d_{xy} and $d_{x^2-y^2}$ orbitals (Figure 1) a rationale for how a change of the axial ligand field can affect the equatorial ligand field must be developed. The simplest explanation is an electrostatic one. As the z axis ligand *decreases* its charge interaction with the iron atom a compensating *increase* in attraction of the equatorial ligands will occur. The only proviso would be that the equatorial ligands can sterically respond to this increased attraction. The radial contraction (or expansion) of a porphyrin can be quite significant[9] and is nicely illustrated by the structural comparison of high-spin FeX(TPP) derivatives with the intermediate-spin $Fe(OClO_3)(TPP)$ as discussed earlier. It seems clear that the crystal field strength of perchlorate must be sufficiently weak that a contracted porphyrin core results. The concomitant increase in the xy crystal field of the porphyrin ligand causes the antibonding $d_{x^2-y^2}$ orbital to split further from the nonbonding d_{xy} orbital and the response of the metal is to depopulate $d_{x^2-y^2}$. In other words, a large tetragonal distortion favors the intermediate-spin state. This is evident in the comparison of high-spin FeBr(TPP)[48] with intermediate-spin $FeBr(S_2CNEt_2)_2$,[63] where the Fe-Br distance is 0.06 Å *longer* in the dithiocarbamate complex. Although it has not been previously recognized, the longer axial bond in the intermediate-spin dithiocarbamate $FeBr(S_2CNEt_2)_2$ is clear evidence for greater tetragonal distortion. A 0.07-Å difference in the axial Fe-Cl bond distances is observed in high-spin FeCl(TPP)[46] and intermediate-spin $FeCl(S_2CNEt_2)_2$;[64] again the longer axial bond is associated with the intermediate-spin complex. These structural results make it tempting to speculate that the solution magnetic behavior of $Fe(OClO_3)(TPP)$ corresponds to small changes in the axial field exerted by the ClO_4^- ligand.

A different argument for the high-spin/intermediate-spin dichotomy has been used in tetraaza macrocyclic complexes of the type FeX(Ph[14]tetraenatoN$_4$).[19] The in-plane ligand field of these smaller rings was assumed to remain constant so that decreasing spin multiplicity was correlated with increasing axial field strength. We believe that just the opposite is true in porphyrin complexes. Indeed, in the series of *six*-coordinate complexes, low-spin $[Fe(Im)_2(TPP)]^+$,[13] high-spin $[Fe(TMSO)_2(TPP)]^+$,[12] and intermediate-spin $[Fe(C(CN)_3)(TPP)]_n$,[74] the axial ligand bond lengths increase dramatically (1.99, 2.08, and 2.32 Å, respectively), reflecting increasing tetragonal distortion.

As mentioned earlier, perchlorate has been placed close to chloride in the spectrochemical series but higher than bromide. Since FeBr(TPP) is high spin the present arguments would place perchlorate at lower field strength than bromide. Such reversals of ligand field strength order according to the specific type of complex used as the criterion are difficult to interpret but we are tempted to speculate that the close approach of the perchlorate to the iron (relative to other perchlorato complexes) may allow the oxygen atom to act as a p_π donor. Such an argument is reasonable since π effects are much more sensitive to distance than σ effects[65] and since the weakest field ligands combine both good π donor effects with weak σ effects.

Cytochrome *c'* Relevance

The cytochromes c' are a group of atypical bacterial hemoproteins which apparently function like the cytochromes c but which structurally and electronically resemble myoglobin in certain aspects of their axial ligation.[66] It is now known that the protein ligation is provided by a single histidine residue but that quite possibly the sixth coordination site is vacant.[69] The cytochromes c' exist in a number of distinct states according to the origin, pH, buffer type, and temperature of the sample. There is consensus from Mössbauer,[67] MCD,[68] and ESR[38] that at least two distinct *high*-spin states exist at and around physiological pH, but in addition Maltempo suggests that an *intermediate*-spin ($S = 3/2, 5/2$ admixture) component exists.[41] The evidence is based on the observation of a new ESR signal, at $g_\perp = 4.77$ in the case of cytochrome c' from *Clostridium*, and the magnetic moment (5.15 μ_B at 0 °C) being lower than that of a pure high-spin species (5.9 μ_B). Our studies strongly support the existence of intermediate-spin ferric hemes which, to a first approximation, can be described as $S = 3/2, 5/2$ admixtures.

The key structural question is what are the axial ligation mode(s) in cytochrome c' which give rise to the different high- and intermediate-spin states. Since both the X-ray structure[69] and the resonance Raman spectrum[24] are consistent with a five-coordinate heme having a single axial histidine there is an obvious challenge for the synthetic analogue method. There is as yet no model compound of the type $[Fe(Im)(TPP)]^+$ to investigate the spin state of this ligation mode. Since six-coordinate metHb(H_2O) is high spin the five-coordinate species with its lower axial ligand field can be expected to be approaching the high/intermediate spin crossover point. A six-coordinate heme having some protein-induced histidine constraint which slightly lowered its ligand field strength is also quite reasonable and would be consistent with the high sensitivity of the spin state of cytochrome c' to its environment (pH, buffer, species, etc.). Lack of histidine N-H···O hydrogen bonding,[69] tilting of the histidine plane with respect to that of the porphyrin, or rotation of the projected histidine plane to a position coincident with two porphinato nitrogen atoms (to raise the $d_{x^2-y^2}$ orbital energy and introduce a steric bond-weakening effect) can be envisaged.

Another intriguing but highly speculative possibility for the intermediate-spin ligation mode of cytochrome c' arises from the fortuitous discovery in this work that the axial ligand field must be similar to that of the perchlorate ion. Fission of the $Fe-N_{hist}$ bond and coordination to a weak field anionic oxygen donor in the other axial site could give rise to this situation. Such a possibility has been recently documented in a mutant hemoglobin where a distal tyrosinate rather than the normal proximal histidine is coordinated to Fe(III) in Hb M Boston.[70] This proposal has the advantage of explaining the reluctance of cytochrome c' to bind exogenous anionic ligands in its ferric state.

In summary, we believe that the reality of admixed intermediate-spin ferric hemoproteins deserves wide acceptance and that, as suggested by Maltempo,[41] a weak field axial ligation mode is responsible for the spin state.[71]

Conclusion

Manipulation of the axial ligand field of a ferric porphyrin leads to spin states which change in a rational manner and each new class of complexes discovered is instructive in under-

standing some aspect of hemoprotein structure. In the present work the series of mixed $S = 3/2, 5/2$ intermediate-spin complexes exemplified by $Fe(OClO_3)(TPP)$ shows many interesting new magnetic and structural properties which relate to the cytochromes c'. Our current attention is turning toward better cytochrome c' models, cytochrome c analogues,[73] and cytochrome oxidase models.[37]

Acknowledgment. We thank Professor F. Raymond Salemme for permission to quote results from his cytochrome c' structure prior to publication and Professor Richard E. Dickerson for suggestions regarding histidine ring orientation. We are also pleased to acknowledge support from the National Science Foundation, CHE-78-09813 (C.A.R.), the National Institutes of Health, HL-15627 (W.R.S.), GM-23851 (C.A.R.), and HL 16860 (G.L.), the Alfred P. Sloan Foundation (C.A.R.), and the Camille and Henry Dreyfus Foundation (C.A.R.).

Supplementary Material Available: Table III, rigid group parameters for the *m*-xylene solvate, and structure factor amplitudes (×10) (24 pages). Ordering information is given on any current masthead page.

References and Notes

(1) University of Southern California.
(2) University of Notre Dame.
(3) Pennsylvania State University.
(4) Steffen, W. L.; Chun, H. K.; Hoard, J. L.; Reed, C. A. "Abstracts of Papers", 175th National Meeting of the American Chemical Society, Anaheim, Calif., March 1978; American Chemical Society: Washington, D.C., 1978; INOR 15.
(5) Collman, J. P.; Hoard, J. L.; Kim, N.; Lang, G.; Reed, C. A. *J. Am. Chem. Soc.* **1975,** *97*, 2676–2681.
(6) (a) Collman, J.P.; Kim, N.; Hoard, J. L.; Lang, G.; Radonovich, L. J.; Reed, C. A. "Abstracts of Papers", 167th National Meeting of the American Chemical Society, Los Angeles, Calif., April 1974; American Chemical Society: Washington, D.C., 1974; INOR 29. (b) Buckingham, D. A.; Collman, J. P.; Hoard, J. L.; Lang, G.; Radonovich, L. J.; Reed, C. A.; Robinson, W. T. To be submitted for publication.
(7) Other abbreviations used in this paper: 1-MeIm = 1-methylimidazole; 2-MeIm = 2-methylimidazole; Im = imidazole; RS = a thiolate anion; R_2SO = a sulfoxide; T*m*TP = dianion of *meso*-tetra-*m*-tolylporphyrin; OEP = dianion of octaethylporphyrin; 2-MeTHF = 2-methyltetrahydrofuran; py = pyridine; mesoP = dianion of mesoporphyrin IX dimethyl ester.
(8) Hoard, J. L. *Science* **1971,** *174*, 1295–1302.
(9) Scheidt, W. R. *Acc. Chem. Res.* **1977,** *10*, 339–345.
(10) Reed, C. A. "Metal Ions in Biological Systems", Vol. 7; Sigel, H., Ed.; Marcel Dekker: New York, 1978; Chapter 7.
(11) Tang, S. C.; Koch, S.; Papaefthymiou, G. C.; Foner, S.; Frankel, R. B.; Ibers, J. A.; Holm, R. H. *J. Am. Chem. Soc.* **1976,** *98*, 2414–2434.
(12) Mashiko, T.; Kastner, M. E.; Spartalian, K.; Scheidt, W. R.; Reed, C. A. *J. Am. Chem. Soc.* **1978,** *100*, 6354–6362.
(13) Collins, D. M.; Countryman, R.; Hoard, J. L. *J. Am. Chem. Soc.* **1972,** *94*, 2066–2072.
(14) Kastner, M. E.; Scheidt, W. R.; Mashiko, T. M.; Reed, C. A. *J. Am. Chem. Soc.* **1978,** *100*, 666–667.
(15) Dolphin, D. H.; Sams, R. J.; Tsin, T. B. *Inorg. Chem.* **1977,** *16*, 711–713.
(16) Maltempo, M. M.; Moss, T. H.; Cusanovich, M. A. *Biochim. Biophys. Acta* **1974,** *342*, 290–305.
(17) Leigh, J. S.; Maltempo, M. M.; Ohlsson, P. I.; Paul, K. G. *FEBS Lett.* **1975,** *51*, 304–308.
(18) Griffith, J. S. "The Theory of Transition Metal Ions", Cambridge University Press: New York, 1961; p 369.
(19) Kock, S.; Holm, R. H.; Frankel, B. R. *J. Am. Chem. Soc.* **1975,** *97*, 6714–6723.
(20) Wickman, H. H.; Trozzolo, A. M. *Inorg. Chem.* **1968,** *7*, 63–68.
(21) Epstein, L. M.; Straub, D. K. *Inorg. Chem.* **1969,** *8*, 560–562.
(22) Butcher, R. J.; Sinn, E. *J. Am. Chem. Soc.* **1976,** *98*, 2440–2449.
(23) Ogoshi, H.; Watanabe, E.; Yoshida, Z. *Chem. Lett.* **1973,** 989–992.
(24) Spiro, T. G.; Stong, J. D.; Stein, P. *J. Am. Chem. Soc.*, in press.
(25) (a) Spaulding, L. D.; Chang, C. C.; Yu, N-T.; Felton, R. H. *J. Am. Chem. Soc.* **1975,** *97*, 2517–2525. (b) Warshal, A. *Annu. Rev. Biophys. Bioeng.* **1976,** *6*, 273–300.
(26) Spiro, T. G.; Strekas, T. C. *J. Am. Chem. Soc.* **1974,** *96*, 338–345.
(27) Fleischer, E. B.; Palmer, J. M.; Srivastava, T. S.; Chatterjee, A. *J. Am. Chem. Soc.* **1971,** *93*, 3162–3167.
(28) Cohen, I. A.; Summerville, D. A.; Su, S. R. *J. Am. Chem. Soc.* **1976,** *98*, 5813–5816.
(29) Crawford, T. H.; Swanson, J. *J. Chem. Educ.* **1971,** *48*, 382–386.
(30) Scheidt, W. R. *J. Am. Chem. Soc.* **1974,** *96*, 84–89.
(31) Locally modified versions of Jacobson's ALFF, Park's REFINE, Busing and Levy's ORFLS and ORFFE, and Johnson's ORTEP II were employed.
(32) Atomic form factors were from Cromer, D. T.; Mann, J. B. *Acta Crystallogr., Sect. A.* **1968,** *24*, 321–323, with real and imaginary corrections for anamolous dispersion in the form factor of the iron and chlorine atoms from Cromer, D. T.; Liberman, D. *J. Chem. Phys.* **1970,** *53*, 1891–1898. Scattering factors for hydrogen were from Stewart, R. F.; Davidson, E. R.; Simpson, W. T. *J. Chem. Phys.* **1965,** *42*, 3175–3187.
(33) Marchon, J. C.; Gans, P. Personal communication.
(34) Collman, J. P.; Reed, C. A. *J. Am. Chem. Soc.* **1973,** *95*, 2048–2049.
(35) Kirner, J. F.; Hoard, J. L.; Reed, C. A. In ref 4, INOR 14.
(36) Walker, F. A.; Lo, M-W.; Ree, M. T. *J. Am. Chem. Soc.* **1976,** *98*, 5552–5560.
(37) Landrum, J. T.; Reed, C. A.; Hatano, K.; Scheidt, W. R. *J. Am. Chem. Soc.* **1978,** *100*, 3232–3234.
(38) Maltempo, M. M. *J. Chem. Phys.* **1974,** *61*, 2540–2547.
(39) Goff, H.; La Mar, G. N.; Reed, C. A. *J. Am. Chem. Soc.* **1977,** *99*, 3641–3646.
(40) Murray, K. S.; Reed, C. A. Unpublished data.
(41) Maltempo, M. M. *Q. Rev. Biophys.* **1976,** *9*, 181–215.
(42) Lang, G. *Q. Rev. Biophys.* **1970,** *3*, 1–60.
(43) The number in parentheses following this averaged bond parameter, and all other averaged values repeated in the paper, is the estimated standard deviation for the averaged value.
(44) $Fe(OCH_3)$(mesoP): Hoard, J. L.; Hamor, M. J.; Hamor, T. A.; Caugley, W. S. *J. Am. Chem. Soc.* **1965,** *87*, 2312–2319.
(45) FeCl(proto IX): Koenig, D. F. *Acta Crystallogr.* **1965,** *18*, 663–673.
(46) FeCl(TPP): Hoard, J. L.; Cohen, G. H.; Glick, M. D. *J. Am. Chem. Soc.* **1967,** *89*, 1992–1996. Hoard, J. L. Private communication.
(47) $[Fe(TPP)]_2O$: Hoffman, A. B.; Collins, D. M.; Day, V. W.; Fleischer, E. B.; Srivastava, T. S.; Hoard, J. L. *J. Am. Chem. Soc.* **1972,** *94*, 3620–3626.
(48) FeBr(TPP): Skelton, B. W.; White, A. H. *Aust. J. Chem.* **1977,** *30*, 2655–2660.
(49) $[Fe(ODM)]_2O$: Kenny, J., Buchler, J. W.; Scheidt, W. R. Unpublished results.
(50) FeI(TPP): Hatano, K.; Scheidt, W. R. To be submitted for publication.
(51) Fe(NCS)(TPP), Hoard, J. L.; Bloom, A. To be submitted for publication.
(52) $Fe(1\text{-MeIm})_2$(proto IX): Little, R. G.; Dymock, K. R.; Ibers, J. A. *J. Am. Chem. Soc.* **1975,** *97*, 4532–4539.
(53) $Fe(N_3)(py)(TPP)$: Adams, K. M.; Rasmussen, P. G.; Hatano, K.; Scheidt, W. R. To be submitted for publication.
(54) Sakurai, T.; Yamamoto, K.; Naito, H.; Nakamoto, N. *Bull. Chem. Soc. Jpn.* **1976,** *49*, 3042–3046.
(55) Kastner, M. E.; Scheidt, W. R. *J. Organomet. Chem.* **1978,** *157*, 109–123.
(56) Spaulding, L. D.; Eller, P. G.; Bertrand, J. A.; Felton, R. H. *J. Am. Chem. Soc.* **1974,** *96*, 982–987.
(57) Scheidt, W. R.; Kastner, M. E.; Hatano, K. *Inorg. Chem.* **1978,** *17*, 706–710.
(58) Scheidt, W. R.; Reed, C. A. *Inorg. Chem.* **1978,** *17*, 710–714.
(59) Kirner, J. F.; Reed, C. A.; Scheidt, W. R. *J. Am. Chem. Soc.* **1977,** *99*, 1093–1101.
(60) Lever, A. P. B. "Inorganic Electronic Spectroscopy", Elsevier: Amsterdam, 1968; p 348.
(61) Harrowfield, J. MacB.; Sargeson, A. M.; Singh, B.; Sullivan, J. C. *Inorg. Chem.* **1975,** *14*, 2864–2865. Unfortunately, the wavelength of the d–d absorption in $[Co(NH_3)(ClO_4)]^{2+}$ is not reported but the complex is pink like the chloride. Also the closely analogous ReO_4^- complex has its d–d band very close to that of chloride: Lenz, E.; Murmann, R. K. *Inorg. Chem.* **1968,** *7*, 1880–1885.
(62) Harris, G. *Theor. Chim. Acta* **1968,** *10*, 119–154.
(63) Chapps, G. E.; McCann, S. W.; Wickman, H. H.; Sherwood, R. C. *J. Chem. Phys.* **1974,** *60*, 990–997.
(64) Hoskins, B. F.; White, A. H. *J. Chem. Soc. A.* **1970,** 1668–1674.
(65) Gerlock, M.; Slade, R. C. "Ligand Field Parameters", Cambridge University Press: New York, 1973; p 187.
(66) Kamen, M. D.; Horio, T. *Annu. Rev. Biochem.* **1970,** *39*, 673–700.
(67) Emptage, M. H.; Zimmermann, R.; Que, L.; Munck, E.; Hamilton, W. D.; Orme-Johnson, W. H. *Biochim. Biophys. Acta* **1977,** *495*, 12–23.
(68) Rawlings, J.; Stephens, P. J.; Nafie, L. A.; Kamen, M. D. *Biochemistry* **1977,** *16*, 1725–1729.
(69) Salemme, F. R.; Weber, P. Personal communication.
(70) Pulsinelli, P. D.; Perutz, M. F.; Nagel, R. L. *Proc. Natl. Acad. Sci. U.S.A.* **1973,** *70*, 3870–3874.
(71) It is, in principle, possible to argue that some protein-induced increase in the ligand field strength of the porphyrin could cause an intermediate-spin state without a change in the axial ligand. However, the lack of a precedent for this in both protein and model complex work as well as the prevalence of notions of axial ligation tension in hemoglobin[10] makes this much less likely.
(72) Walker, F. A.; La Mar, G. N. *Ann. N.Y. Acad. Sci.* **1974,** *206*, 328–348.
(73) Mashiko, T.; Marchon, J-C; Musser, D.; Reed, C. A.; Kastner, M. E.; Scheidt, W. R. *J. Am. Chem. Soc.*, in press.
(74) Summerville, D. A.; Cohen, I. A.; Hatano, K.; Scheidt, W. R. *Inorg. Chem.* **1978,** *17*, 2906–2910.